Advances in Aircraft and Spacecraft Science, *Vol. 9, No. 5 (2022) 463-477*
https://doi.org/10.12989/aas.2022.9.5.463

About influence of the choice of numerical flow in the DG method for the solution of problems with shock waves

Mikhail M. Krasnov, Marina E. Ladonkina*,
Olga A. Nekliudova and Vladimir F. Tishkin

Keldysh Institute of Applied Mathematics of RAS, Moscow, 125047, Russia

(Received February 20, 2022, Revised August 5, 2022, Accepted September 1, 2022)

Abstract. This study compares various ways of calculating flows for the problems with the presence of shock waves by first-order schemes and higher-order DG method on the tests from the Quirk list, namely: Quirk's problem and its modifications, shock wave diffraction at a 90 degree corner, the problem of double Mach reflection. It is shown that the use of HLLC and Godunov's numerical schemes flows in calculations can lead to instability, the Rusanov-Lax-Friedrichs scheme flow can lead to high dissipation of the solution. The most universal in heavy production calculations are hybrid schemes flows, which allow the suppression of the development of instability and conserve the accuracy of the method.

Keywords: discontinuous Galerkin method; hypersonic gas dynamics; numerical flow

1. Introduction

Finding a numerical solution to the problems of mathematical physics is aimed at obtaining a numerical solution fully adequate to the exact physical solution, so it not only necessitates the usage of a high quality computational grid and a reliable high-precision numerical method but also requires the investigator`s assurance that the chosen numerical method has no failings or shortcomings with regard to the problem to be solved.

Thus, it was detected that a numerical simulation of the supersonic viscous flow around the cruise missile Tomahawk performed using the discontinuous Galerkin (DG) method of the second order of accuracy (Krasnov *et al*. 2017) with the Harten-Lax-van Leer with contact (HLLC) numerical scheme developed instability. The computational domain was represented by a structured grid consisting of 10^7 elements. The incident flow was characterized by the Reynolds number Re of 10^7, and Mach number at $M\infty$=1.3. A low-pressure area in the form of a wedge, perpendicular to the direction of the incident flow, appeared in the solid body fore part. It increased with time, distorted the shock wave, and led to a calculation failure at a fairly early time. This type of instability appears to be caused by a set of conditions similar to the one revealing the instability mechanism known as the carbuncle phenomenon (Peery and Imlay 1988, Rodionov2018): high Reynolds numbers, around 10^7, low dissipative HLLC flow, the first-order accuracy scheme. The calculation was performed using the second-order discontinuous Galerkin

*Corresponding author, Ph.D., E-mail: ladonkina@imamod.ru

http://www.techno-press.org/?journal=aas&subpage=7 ISSN: 2287-528X (Print), 2287-5271 (Online)

method, although in the area behind the shock wave front, the order of the scheme can drop to the first order of accuracy (Ladonkina *et al*. 2018). A similar calculation using Rusanov-Lax-Friedrichs numerical scheme did not result in forming such instability, although the high dissipativity of the flow created more diffuse regions. Two more calculations were carried out with new hybrid numerical schemes (Krasnov *et al*. 2017). Both proposed flows ensured stable operation in the calculations, made it possible to avoid the occurrence of instabilities, preserved the shock wave accuracy and structure, and showed good solution accuracy in the boundary layer.

A large number of works are devoted to the study of the "carbuncle" type instability, the occurrence of which affects the profile of the shock wave front (Rodionov 2019, Pandolfi 2001, Dumbser 2004, Roe 2005, Menart 2008, Kitamura 2013, Xie 2017, Gressier 2000). One of the established causes of this instability type are the numerical schemes used to perform calculations. As is known, low dissipation flows are the most susceptible to this instability, and the use of highly dissipative flows makes it possible to avoid the occurrence of the carbuncle phenomenon. For this reason, several attempts have been made to develop new methods that suppress the development of instabilities while ensuring low dissipativity (Nishikawa 2008, Guo 2018, Hu 2014, Ferrero 2019).

The purpose of the present paper is to investigate the shock-wave instability of some specific numerical schemes implemented in the RAMEG3D software package (Krasnov 2021). This instability type is tested on some of the Quirk`s catalogue test problems (Quirk 1994). We followed the formulations given in the work of Rodionov (2019). In this paper, we study first-order numerical schemes and second-order DG schemes with numerical Godunov (1959), HLLC, Rusanov-Lax-Friedrichs and hybrid flows used in our calculations.

2. Numerical schemes corresponding to the system of Euler equations

Let us consider Euler equations in a two-dimensional case

$$\partial_t \mathbf{U} + \nabla \cdot \mathbf{F}(\mathbf{U}) = 0, \tag{1}$$

where **U**-is the vector of conservative variables and **F(U)**-are the components of the flux function. To determine the pressure, we will use the ideal gas equation.

An approximate solution to system Eq. (1) in the discontinuous Galerkin method is sought as a solution to the following system (Cockburn 1998, Bassiand Rebay 2002)

$$\frac{d}{dt}\int_{T_j} \phi_k(\mathbf{x})\mathbf{U}_h(\mathbf{x},t)d\Omega + \oint_{\partial T_j} \phi_k(\mathbf{x}) \cdot \mathbf{h}_F(\mathbf{U}_h^+, \mathbf{U}_h^-, \mathbf{n})\, d\sigma - \\ - \int_{T_j} \left(\frac{\partial \phi_k(\mathbf{x})}{\partial x}\mathbf{F}_x\big(\mathbf{U}_h(\mathbf{x},t)\big) + \frac{\partial \phi_k(\mathbf{x})}{\partial y}\mathbf{F}_y\big(\mathbf{U}_h(\mathbf{x},t)\big) \right) d\Omega = 0, \tag{2}$$

Eq. (2) is written on the grid element T_j therefore, the index j is omitted in the coefficients and basic functions. $\mathbf{U}_h(\mathbf{x},t)$-is the solution vector, n-the vector of the outer unit normal to the element boundary ∂T_j, $\mathbf{h}_F(\mathbf{U}_h^+, \mathbf{U}_h^-, \mathbf{n})$-flux functions computed on the ∂T_j element border. The quantities denoted by $\mathbf{U}_h^-$ are calculated at the border ∂T_j of the element T_j by the values inside the element T_j, while the quantities denoted by $\mathbf{U}_h^+$, are calculated at the border ∂T_j by the values in the adjacent cell to the element T_j.

To ensure the monotonicity of the solution obtained by this method, a slope limiter (Yasue 2010) or the Cockburn (1998) limiter are used.

In Eq. (2) $\mathbf{h}_F(\mathbf{U}_h^+, \mathbf{U}_h^-, \mathbf{n})$-is the numerical flux function depending on the values of the approximate solution on both sides of the element boundary and on the direction of the unit normal vector $\mathbf{n}$. This function is monotone and satisfies the consistency condition

$$\mathbf{h_F}(\mathbf{U}_h(\mathbf{x}, t), \mathbf{U}_h(\mathbf{x}, t), \mathbf{n}) = \mathbf{F}(\mathbf{U}_h(\mathbf{x}, t)). \tag{3}$$

In our works, while performing numerical simulation using the RAMEG3D software package, most frequently used are the numerical Godunov's scheme, based on the numerical solution of the Riemann problem, the HLLC numerical scheme and the Rusanov-Lax-Friedrichs (RLF) scheme (Krasnov 2017, Ferrero 2019). The purpose of this work is to test these numerical schemes in detail on a series of test problems in order to identify their main properties and areas of application.

It is known that the RLF flow (Eq. (4)) has a higher dissipation compared to the Godunov's and HLLC numerical schemes and ensures the most stable operation of the software package, however, its use can affect the accuracy of the obtained solution by reducing it.

$$\mathbf{h}(\mathbf{U}_h^+, \mathbf{U}_h^-, \mathbf{n})\frac{1}{2}\left(\mathbf{F}(\mathbf{U}_h^+) + \mathbf{F}(\mathbf{U}_h^-) - A \cdot (\mathbf{U}_h^+ - \mathbf{U}_h^-)\right)_F$$
$$A = \max\left(\left|\mathbf{v}^+\right| + c^+,\ \left|\mathbf{v}^-\right| + c^-\right), \tag{4}$$

Here we use the notation introduced above, where c^+- is the speed of sound calculated on the border ∂T_j of the T_j element from the values inside the element T_j, c^-- is the speed of sound calculated on the border ∂T_j on the base of the values in the cell adjacent to this element, $\mathbf{v}$- is the speed.

A hybrid numerical scheme was constructed in the paper of Krasnov (2017), based on the main idea proposed in the paper of Ferrero (2019). This scheme is a linear combination of one of the flows (HLLC or Godunov's scheme) and of a stable Rusanov-Lax-Friedrichs (RLF) scheme. The direction of the velocity jump determines the normal to the shock wave: when the cell boundary coincides with the shock wave front, the Godunov's flow ($\mathbf{F}^{Godunov}$) is used, and when the interface is perpendicular to the shock wave, the Rusanov-Lax-Friedrichs scheme ($\mathbf{F}^{RLF}$) is used. Thus, the dissipation in the direction coinciding with the shock wave increases and the instability is eliminated.

$$\hat{\mathbf{F}} = \theta\mathbf{F}^{HLLC} + (1-\theta)\mathbf{F}^{RLF}, \tag{5}$$

$$\hat{\mathbf{F}} = \theta\mathbf{F}^{Godunov} + (1-\theta)\mathbf{F}^{RLF} \tag{6}$$

$$\text{где}\theta = \begin{cases} \frac{|\Delta u \cdot n|}{|\Delta u|} = \frac{|\Delta u n_x + \Delta v n_y + \Delta w n_z|}{\sqrt{\Delta u^2 + \Delta v^2 + \Delta w^2}}, & |\Delta u| > \varepsilon, \\ 1, & |\Delta u| \le \varepsilon, \end{cases} \tag{7}$$

whereε is a small constant used to avoid division by zero (for example $\varepsilon = 10^{-6}$), n is the normal to the cell boundary, and $\Delta\mathbf{v} = (u_L\text{-}\, u_R, v_L\text{-}\, v_R)$is the velocity vector jump across the boundary. The parameter θ is calculated from the normal to the cell boundary and the velocity jump across the surface of the cell boundary.

Another approach to constructing a hybrid flow is to add a dissipative term in areas where it is necessary.

To construct it, we go over to the local coordinate system with the unit vector $(\mathbf{n}, \boldsymbol{\tau}_1, \boldsymbol{\tau}_2)$, where $\mathbf{n}$-is the outward normal vector to the surface through which the flow goes, $\boldsymbol{\tau}_1, \boldsymbol{\tau}_2$- are any unit vectors orthogonal to each other lying on this surface. Vectors **U** and **F** in this coordinate system (denoted by the subscript *) will look as follows

$$\begin{aligned} \mathbf{U}^* &= \left(\rho, \rho(\mathbf{u},\mathbf{n}), \rho(\mathbf{u},\boldsymbol{\tau}_1), \rho(\mathbf{u},\boldsymbol{\tau}_1), E\right)^T, \\ \mathbf{F}^*(\mathbf{U}) &= \left(\rho(\mathbf{u},\mathbf{n}), \rho(\mathbf{u},\mathbf{n})u_n + p, \rho(\mathbf{u},\mathbf{n})u_{\tau_1}, \rho(\mathbf{u},\mathbf{n})u_{\tau_2}, (E+p)(\mathbf{u},\mathbf{n})\right), \end{aligned} \tag{8}$$

In order to obtain a new flow with greater dissipation than Godunov's scheme (HLLC) and less dissipation than RLF scheme, we will choose some speed W in the original coordinate system and switch to an inertial reference frame moving with this speed.

Let $W_{\max}$ denote the maximum velocity and $W_{\min}$ the minimum velocity (taking into account the sign) of the waves generated by Riemann problem in the case of using Godunov's flow (or when using the HLLC scheme). Note that if W is greater than $W_{\max}$, then the values of the gas-dynamic quantities will coincide with **U**+ and, after recalculation into the original coordinate system, this scheme will be equal for the usage of Godunov's scheme and the HLLC scheme respectively.

$$\hat{\mathbf{F}} = \mathbf{F}^{*Godunov}(\mathbf{U}^{*+}) - W\mathbf{U}^{*+}, \hat{\mathbf{F}} = \mathbf{F}^{*HLLC}(\mathbf{U}^{*+}) - W\mathbf{U}^{*+}$$

Accordingly, if -W is less than $W_{\min}$, then the values of the gas-dynamic quantities will coincide with **U**- and, after recalculation to the original coordinate system, this flow will be equal to

$$\hat{\mathbf{F}} = \mathbf{F}^{*Godunov}(\mathbf{U}^{*-}) + W\mathbf{U}^{*-}, \hat{\mathbf{F}} = \mathbf{F}^{*HLLC}(\mathbf{U}^{*-}) + W\mathbf{U}^{*-}$$

Taking half the sum of these flows, we get the RLF scheme. If W=0, then Godunov schemes (or HLLC) are obtained accordingly. Thus, if 0<W<W*max, where $W_{\max}^{*(|W_{\max}|||W_{\min}||||)}$ we get a new scheme that is average between the Godunov's scheme (HLLC) and the RLF scheme and has more dissipation than the Godunov's flow (HLLC) and less dissipation than the RLF scheme. This type of flow was considered in the work of Woodward and Colella (1984).

The hybrid flow which we used can be obtained as follows. Let us consider an inertial coordinate system moving at a speed $W \cdot \mathbf{n}$ relative to the original coordinate system and we will calculate Godunov's scheme flow or HLLC, which we will after that recalculate in the original coordinate system. The resulting value will be denoted by $\mathbf{U}^{*+}$. We will carry out a similar procedure with speed and denote the corresponding value as $\mathbf{U}^{*-}$. Taking half the sum of such flows, we arrive at the formulas

$$\hat{\mathbf{F}} = \frac{\mathbf{F}^{*Godunov}(\mathbf{U}^{*+}) + \mathbf{F}^{*Godunov}(\mathbf{U}^{*-})}{2} - W\frac{\mathbf{U}^{*+} + \mathbf{U}^{*-}}{2} \tag{9}$$

$$\hat{\mathbf{F}} = \frac{\mathbf{F}^{*HLLC}(\mathbf{U}^{*+}) + \mathbf{F}^{*HLLC}(\mathbf{U}^{*-})}{2} - W\frac{\mathbf{U}^{*+} + \mathbf{U}^{*-}}{2} \tag{10}$$

$$W = \theta W^*, \quad W^* = max(|u+c|, |u-c|) \tag{11}$$

$$\theta = \begin{cases} M \le M_{min}, & W = W^*, \\ M_{min} < M < M_{max}, & W = \frac{M_{max} - M}{M_{max} - M_{min}} W^*, \\ M \ge M_{max}, & W = 0 \end{cases} \tag{12}$$

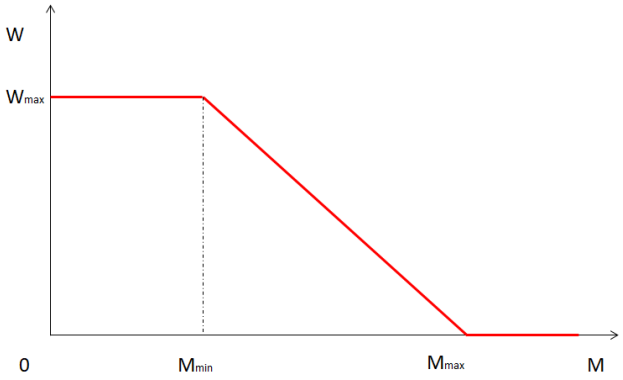

Fig. 1 Dependence of W from M for θ in Eq. (12)

Where W^*-is the maximum of modules for $\frac{\partial \mathbf{F}^*(\mathbf{U})}{\partial \mathbf{U}^*}$ matrix`s eigenvalues and θ is a parameter from Ferrero and D'Ambrosio (2019).

3. Test calculations

In order to test various numerical schemes used in the RAMEG3D software package, a study on a series of two-dimensional test problems was carried out. These problems were described in detail in the papers of Quirk (1992) and Rodionov (2019) devoted to the research of carbuncle instability. Throughout the present paper we will use the following acronyms for the first-order schemes: P0God for the Godunov scheme flow, P0HLLC for the HLLC scheme flow, P0RLF for the Rusanov-Lax-Friedrichs scheme flow, P0Hyb1 for the type 1 hybrid scheme flow, P0Hyb2 for the type 2 hybrid scheme flow with parameter from Eq. 12, P0HybT for the type 2hybrid scheme flow with parameter from Eq. (7), and for DG method with linear basis functions: P1God, P1HLLC, P1RLF, P1Hyb1, P1Hyb2, P1HybT, respectively.

3.1 Problem 1. Quirk`s test problem and its modifications

In the Quirk`s test problem a shock wave propagating along a rectangular channel is calculated. The computational area [0, 800]×[0, 20] in the xy plane is covered with a regular grid which consists of square cells with the space step hx=hy=1. The instability of the plane shock wave is initiated by a small perturbation of one horizontal central line of the grid: $y_{i,jmid}^{new} = y_{i,jmid} + \delta(-1)^i$, where i,j are grid indices, in longitudinal and transverse sections, $jmid$=10, δ=10-6. The initial state of the gas in the computational domain, i.e., density, pressure and velocity, is given by $(\rho_0, p_0, u_{x0}, u_{y0}) = (1,1,0,0)$. The impermeability condition is set on the upper and lower boundaries of the grid. On the left, at x=0, the inflow condition is set with parameters (ρ, p, u_x, u_y), which are determined by the Mach number $M_s = 6$ and the adiabatic exponent $\gamma = 1{,}4$.

$$u_1 = u_s \frac{2(M_s^2 - 1)}{(\gamma + 1)M_s^2}, \quad \rho_1 = \frac{(\gamma + 1)M_s^2}{(\gamma - 1)M_s^2 + 2}, \quad p_1 = \frac{2\gamma M_s^2 - (\gamma - 1)}{(\gamma + 1)},$$

where $u_s = \sqrt{\gamma} M_s$ is the velocity of propagation of the shock wave through the stationary gas.

In this problem the emerging instability can be clearly defined visually when the calculation is performed using the P0God scheme (Fig. 2). The same figure shows the calculations results for the P0RL and P0Hyb schemes. The degree of deviation of the solution from the one-dimensional flow along the density contours cannot be defined neither in these figures nor in the graphs provided by the other computational schemes. In conformity with the work of Rodionov (2019), the degree of deviation of the solution from the one-dimensional flow will be determined by the formulas

$$\varepsilon_0 = \max_{i,j}\left(\left|\rho_{i,j} - \bar{\rho}_i\right|\right), \quad \bar{\rho}_i = \frac{1}{J}\sum_{j=1}^{J} \rho_{i,j}$$

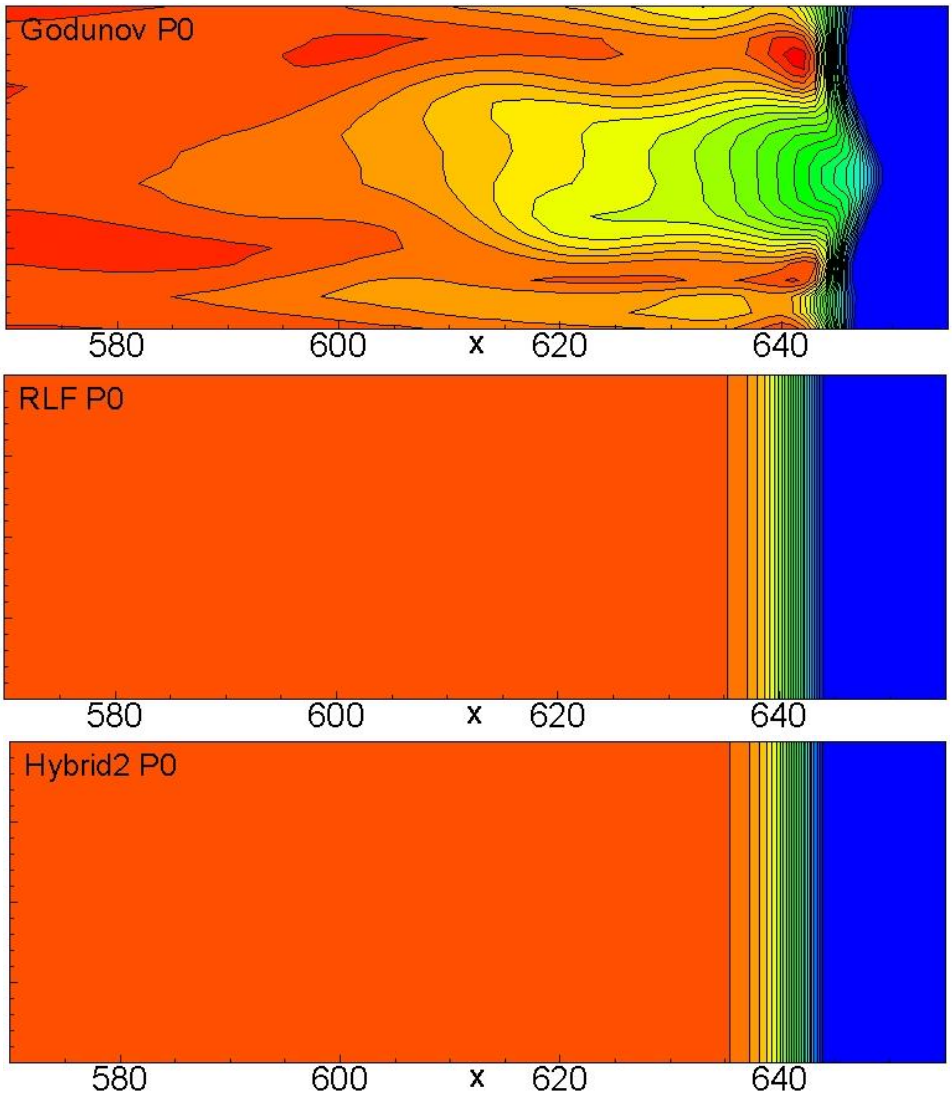

Fig. 2 Problem 1.Density isolines from 1.5 to 5.5 with a step of 0.16

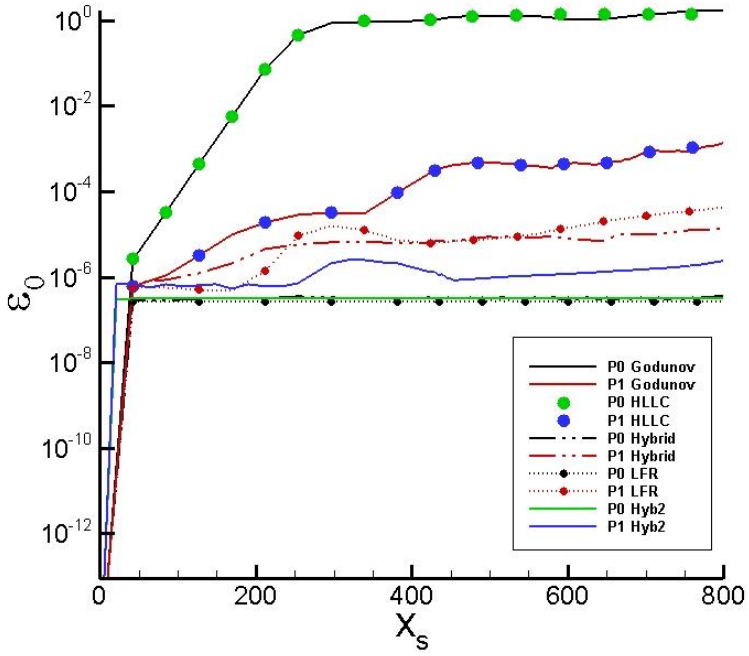

Fig. 3 Problem 1. Dependence in P0 and P1 schemes with Godunov, HLLC, Rusanov-Lax-Friedrichs, Hybrid type 1, Hybrid type 2 numerical flows

Fig. 3 shows the values $\varepsilon_0(\mathrm{x}_s)$, where x_s is the distance traveled by the shock wave $\mathrm{x}_s = u_s t, \quad u_s = \sqrt{\gamma} M_s$ for the first- and second-order schemes with different numerical flows for the same Quirk problem 1 with the Mach number $M_s = 6$.

The calculations performed using the P0God and P0HLLC schemes, respectively, P1God and P1HLLC virtually coincide and display the fastest growth rate of shock wave disturbance. The smallest deviation from the one-dimensional flow was shown by the schemes of both the first and the second order with the type 2 hybrid numerical flow P0Hyb2, P1Hyb2, P0RLF, P0Hyb. For the P1God and P1HLLC second-order schemes, the largest deviation is observed near the moment when the shock wave passes the point x_s=500, although this deviation is not determined in the graphs with density contours.

For the problem 2 the computational domain differs from the domain in problem 1. This difference is due to the size increase in the y direction: [0, 800]×[0, 50]. The grid remains regular and it consists of square cells (*hx*=*hy*=1). As a modification to Problem 1, the method of initiating shock wave instabilities is changed: a perturbed vertical boundary is added $x_{i0,j}^{new} = x_{i0,j} + \delta\left(2RND_j - 1\right)$, where *i*=*i*0=10 are grid indices in the cross section and RND_j (built-in function RAND was used from *C* language library) are random numbers generated within the interval [0, 1], δ=10-4. The condition of periodic flow is set on the upper and lower boundaries of the computational area.

In problem 3 boundary conditions introduce a change into the computational domain so that it differs from the one in the previous Problem 2. On the left boundary *x*=0 the impermeable wall condition is set, on the right boundary *x*=800 there is an inflowing flow with the parameters $\left(\rho, p, -u_x, u_y\right)$ taken from the first problem.

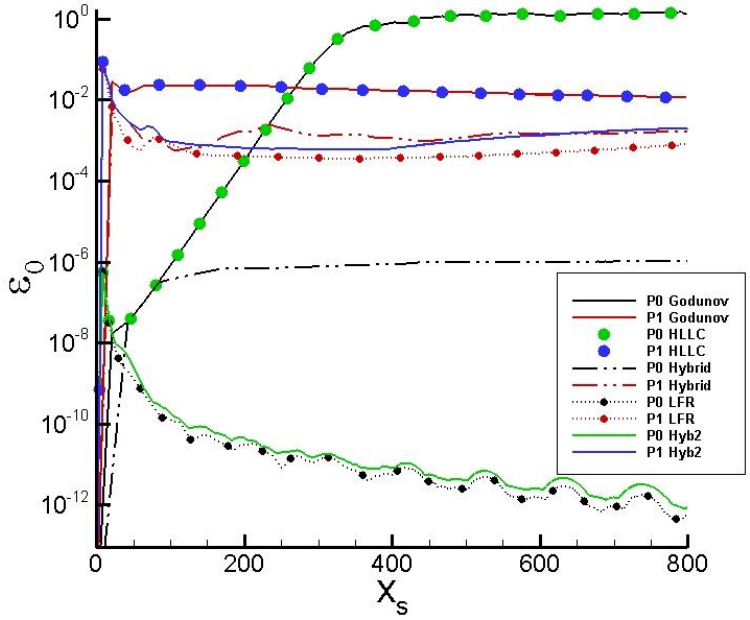

Fig. 4 Problem 2. Dependence in schemes P0 and P1 by numerical flows of Godunov, HLLC, Rusanov-Lax-Friedrichs, Hybrid type 1, Hybrid type 2numerical flows

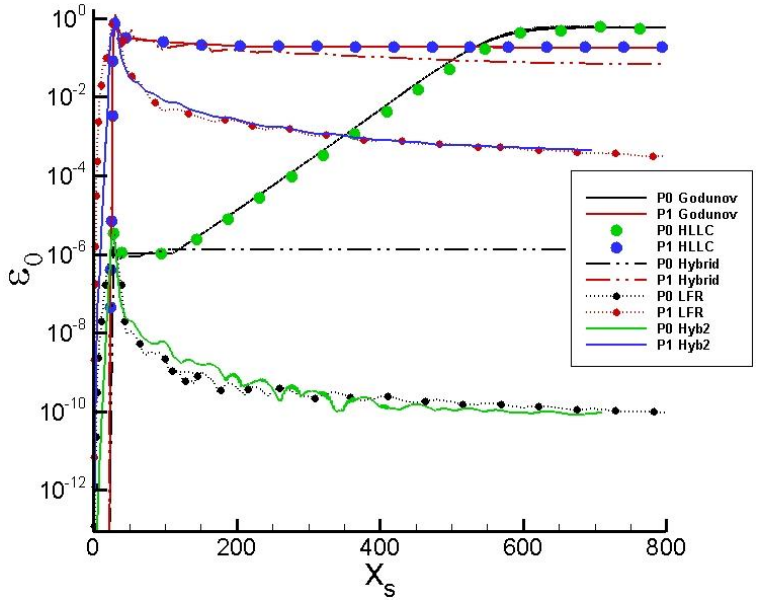

Fig. 5 Problem 3. Dependence in P0 and P1 schemes with Godunov, HLLC, Rusanov-Lax-Friedrichs, Hybrid type 1, Hybrid type 2 numerical flows

The results obtained for the problems 1-3 are fully consistent with each other. Note that if we compare first-order schemes with each other, we can see that the largest deviation is observed while using Godunov`s scheme flow, HLLC, i.e., low dissipation flows. Rusanov-Lax-Friedrichs

scheme flow shows the smallest deviation, which is logically due to the high dissipativity of the flow. The same results are observed when using a type 2 hybrid scheme flow. For second-order schemes, the picture changes: almost all schemes showed a high probability of instabilities, due to a higher order of the scheme accuracy. Moreover, schemes with numerical Godunov and HLLC schemes flows, as well as type 1 hybrid scheme flow are most susceptible to instability. Just as in the case of using first-order schemes, the P1RLF and P1Hyb2 schemes are less prone to instabilities.

3.2 Problem 4. Double mach reflection problem

The computational domain in the xy plane has the form of a rectangle [0, 1.5]×[0, 1] cut off by a straight line $y=(x-0.075)\ tg(30°)$. It is covered with a regular grid with $J\times I=800\times800$ cells. The initial state of an ideal gas $\gamma=1.4$ in the computational domain is the following: $(\rho, p, ux, uy)=(1, 1/\gamma, 0, 0)$. On the left boundary of the region, the boundary conditions of a freely inflowing flow are set with parameters corresponding to the Mach number $M_s = 5{,}5$, On the right boundary $x=1.5$, lower $y=(x-0.075)\ tg(30°)$ and upper $y=1$ boundaries of the region, the impermeability condition is set. The test is calculated up to the time $t=0.18$.

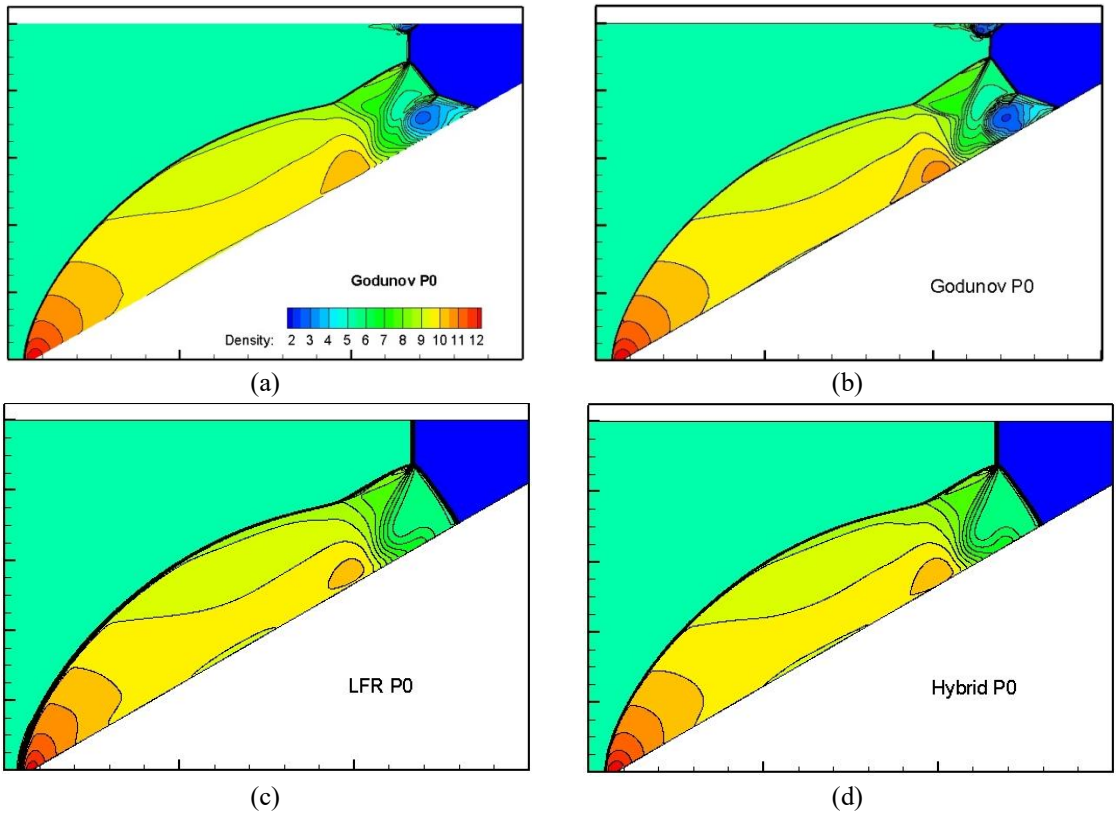

Fig. 6 Problem 4. Density isolines from 2 to 12 with a step of 0.5 (a)-(f)-calculations performed on constant polynomials (P0), (g)-(j)-calculations performed on linear polynomials (P1), (b),(f), -on grids 1600×1600

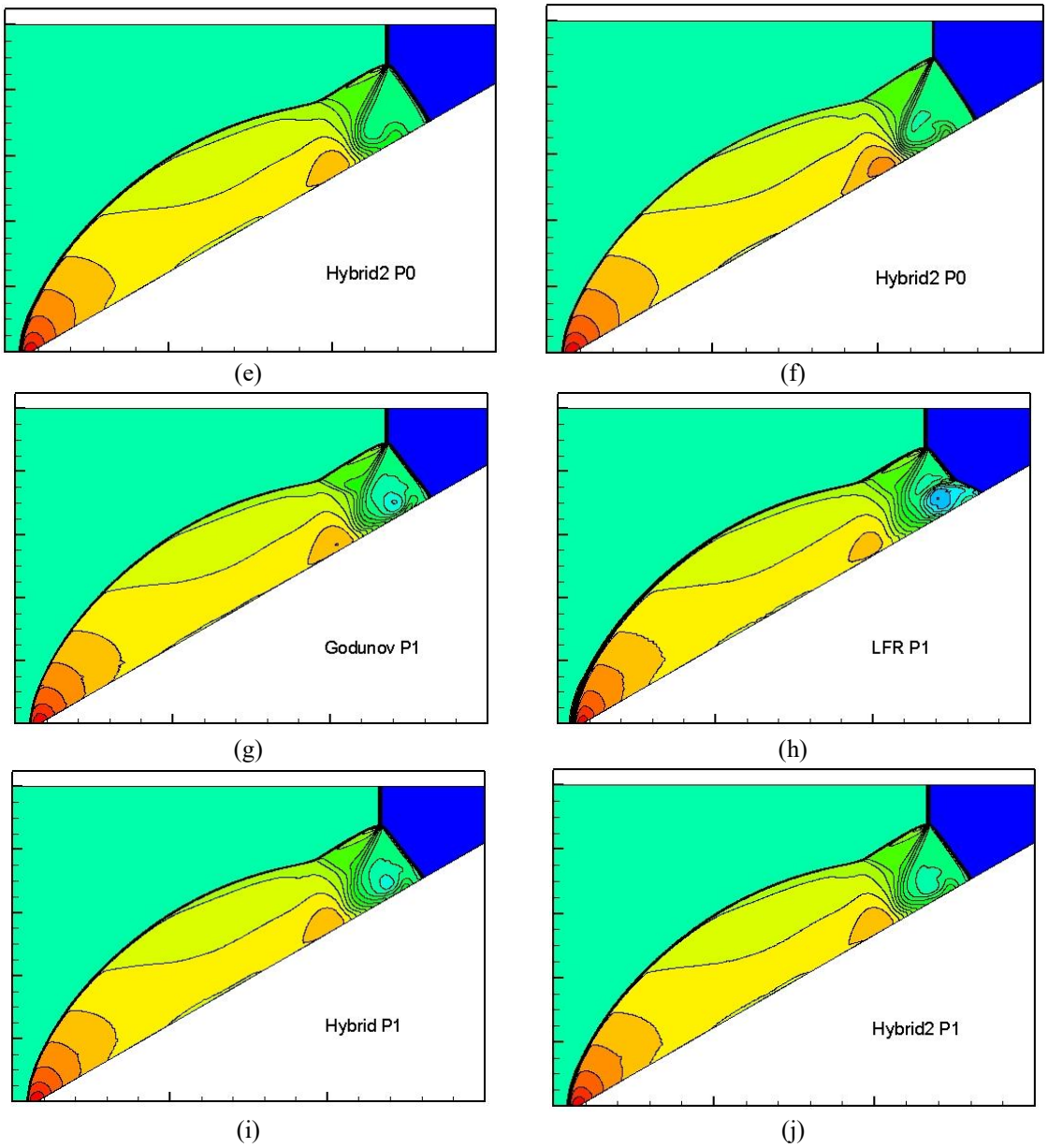

Fig. 6 Continued

Fig. 6 shows the calculations results for this problem with different numerical flows. While performing the calculations with the first-order schemes, instability occurs while using Godunov and HLLC flows; however, the occurrence of instabilities is not observed while using the RLF flow and hybrid flows. It is noteworthy that shock and reflected waves have clearer profiles than while using the RLF flow. When calculating the second-order DGM with the use of P1RLF scheme, one can note the occurrence of instability, which a decrease in the time step does not make disappear. We do not fully understand this fact, perhaps this could be related to the increase

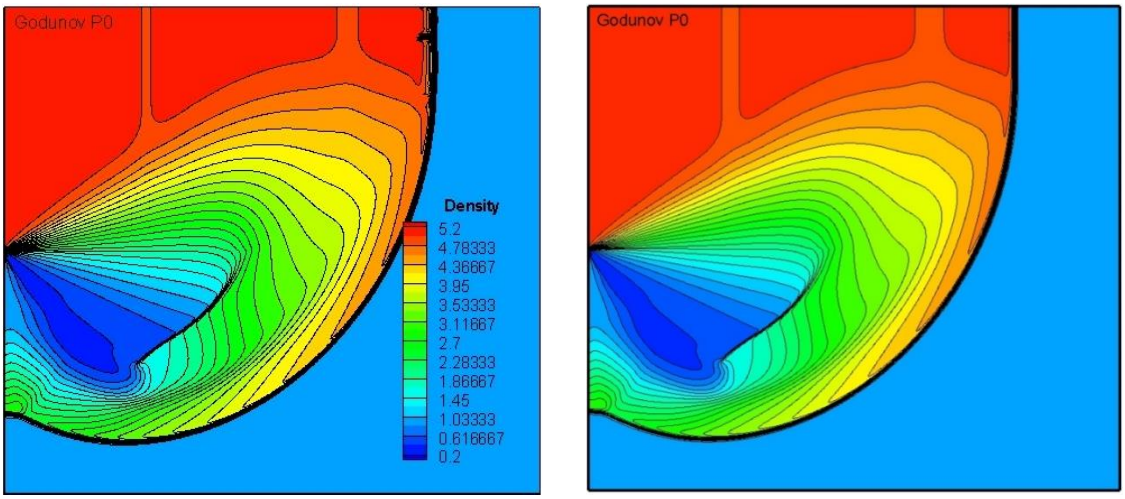

(a) (b)

Fig. 7 Problem 5. 25density isolines from 0.2 to 5.2 using P0God scheme

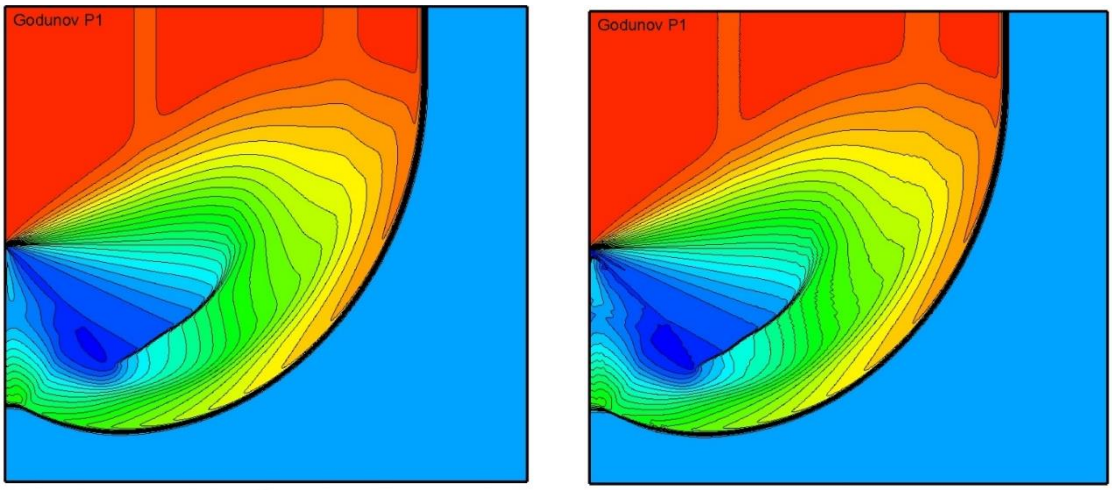

(a) (b)

Fig. 8 Problem 5. 25 density isolines from 0.2 to 5.2 for calculations performed with P1God scheme on the 1/600 grid

in the scheme order due to linear polynomials. Rodionov (2021) in his paper mentions the possibility of such instability type to occur when the researcher uses higher than first order numerical schemes.

3.3 Problem 5. Diffraction of a strong shock wave around a 90-degree corner

Another problem from Quirk's (1992) work appears to be the calculation of shock wave diffraction around a 90-degree corner. The computational area has the size of [0, 1]×[0, 1] in the *xy* plane and it is covered with a regular grid with $J \times I = 600 \times 600$; the initial state of the gas ($\gamma = 1.4$) in

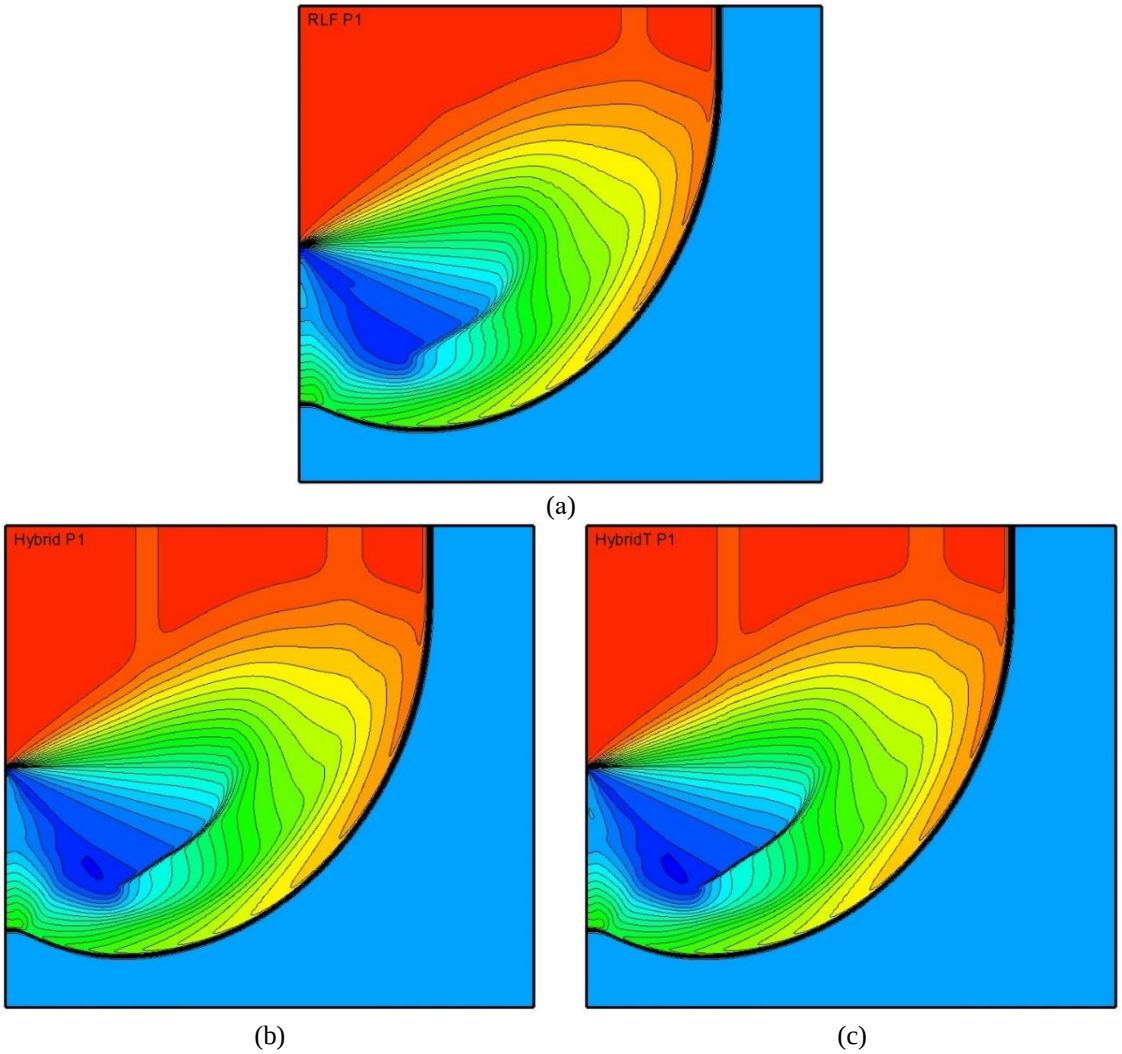

Fig. 9 Problem 5. 25 density isolines from 0.2 to 5.2 for calculations performed with P1RLF, P1Hyb, P1Hyb2 schemes

the computational domain being (ρ, p, ux, uy)=(1, 1/γ, 0, 0). In the upper y=1, lower y=0, right x=1 parts of the boundary, the impermeability condition is set. At the left boundary x=0: in the lower part of the left boundary (y<0.5) an impermeable wall is set, in the upper part of the left boundary (y>0.5) an inflow flow is set with the parameters corresponding to the shock-wave Mach number M_S=5.09. The problem is calculated up to the time t=0.8/M_S.

When the calculations of this problem are performed according to the P0GodGodunov schemes (Fig. 7(a)), instability is formed on the shock wave, where the plane shock wave is aligned with the grid. This result is in line with the calculations results obtained by many authors. But when the time step is reduced by a factor of two, this instability disappears (Fig. 7(b)). When this series of calculations is repeated on a grid reduced by a factor of two in all directions, instability occurs inevitably; no matter what the Courant numbers are (Fig. 7(c), 7(d)).

Such instability is not observed, however, while performing calculations according to P1God (Figs. 8(a), 8(b)), even with the use of limiters with different degrees of limitation.

No instability was observed for the calculations performed with both the first and the second order schemes P0RLF, P0Hyb, P0Hyb2 (not shown in the figures), P1RLF, P1Hyb, and P1Hyb2, using different options for determining the parameter θ. Fig. 9 shows that calculations using P1Hyb, P1HybT give more distinct shock wave fronts and a more accurate flow pattern than while using P1RLF.

4. Conclusions

In the present paper a study of various numerical flows for the simulations of flows with shockwaves has been undertaken. Computation results for a number of test problems from the Quirk`s catalogue of failings are in line with the results obtained by other authors. Using Godunov's or HLLC flow in calculations can lead to instability, while using Rusanov-Lax-Friedrichs flow can lead to high dissipativity of the calculation. It is shown that the use of hybrid flows makes it possible to suppress the development of instability and preserve the accuracy of the method.

Acknowledgments

The research described in this paper was financially supported by the Russian Science Foundation (grant No. 21-11-00198)

The calculations were performed on a hybrid supercomputer K-60 at the KIAM RAS (Keldysh Institute of Applied Mathematics of the Russian Academy of Sciences) Collective Usage Centre.

References

Bassi, F. and Rebay, S. (2002), "Numerical evaluation of two discontinuous Galerkin methods for the compressible Navier-Stokes equations", *Int. J. Numer. Meth. Fluid.*, **40**, 197-207. https://doi.org/10.1002/fld.338.

Cockburn, B. (1998), "An introduction to the discontinuous Galerkin method for convection-dominated problems, advanced numerical approximation of nonlinear hyperbolic equations", *Adv. Numer. Approx. Nonlin. Hyperbol. Eq.*, 150-268. https://doi.org/10.1007/BFb0096353.

Dumbser, M., Moschetta, J.M. and Gressier, J. (2004), "A matrix stability analysis of the carbuncle phenomenon", *J. Comput. Phys.*, **197**, 647-670. https://doi.org/10.1016/j.jcp.2003.12.013.

Ferrero, A. and D'Ambrosio, D. (2019), "An hybrid numerical flux for supersonic flows with application to rocket nozzles", *17TH International Conference of Numerical Analysis and Applied Mathematics*, Rhodes, Greece, September.

Godunov, S.K. (1959), "A finite difference method for the computation of discontinuous solutions of the equations of fluid dynamics", *Sbornik: Math*., **47**(8-9), 357-393.

Gressier, J. and Moschetta, J.M. (2000), "Robustness versus accuracy in shock-wave computations", *Int. J. Numer. Meth. Fluid.*, **33**, 313-332. https://doi.org/10.1002/1097-0363(20000615)33:3<313::AID-FLD7>3.0.CO;2-E.

Guo, S. and Tao, W.Q. (2018), "A hybrid flux splitting method for compressible flow", *Numer. Heat Transf., Part B: Fundament*., **73**, 33-47. https://doi.org/10.1080/10407790.2017.1420315.

Hu, L.J. and Yuan, L. (2014), "A robust hybrid hllc-force scheme for curing numerical shock instability", *Appl. Mech. Mater.*, **577**, 749-753. https://doi.org/10.4028/www.scientific.net/AMM.577.749.

Kitamura, K. and Shima, E. (2013), "Towards shock-stable and accurate hypersonic heating computations: A new pressure flux for AUSM-family schemes", *J. Comput. Phys.*, **245**, 62-83. https://doi.org/10.1016/j.jcp.2013.02.046.

Krasnov, M.M., Kuchugov, P.A., Ladonkina, M.E. and Tishkin, V.F. (2017), "Discontinuous Galerkin method on three-dimensional tetrahedral meshes. The usage of the operator programming method", *Math. Model. Comput. Simul.*, **9**(5), 529-543.

Krasnov, M.M., Ladonkina, M.E. and Tishkin, V.F. (2021), "RAMEG3D software package for numerical simulation of aerothermodynamics problems on high-performance computer systems", Certificate of State Registration of Computer Software №RU20211615026.

Ladonkina, M.E., Nekliudova, O.A., Ostapenko, V.V. and Tishkin, V.F. (2018), "On the accuracy of the discontinuous Galerkin method in the calculation of shock waves", *Comput. Math. Math. Phys.*, **58**(8), 148-156. https://doi.org/10.1134/S0965542518080122.

Lax, P.D. (1954), "Weak solutions of nonlinear hyperbolic equations and their numerical computation", *Commun. Pure Appl. Math.*, **7**(1), 159-193. https://doi.org/10.1002/cpa.3160070112.

Liou, M.S. (1996), "A sequel to AUSM: AUSM+", *J. Comput. Phys.*, **129**, 364-382. https://doi.org/10.1006/jcph.1996.0256.

Menart, J.A. and Henderson, S.J. (2008), "Study of the issues of computational aerothermodynamics using a Riemann solver", AFRL Report 2008-3133.

Nishikawa, H. and Kitamura, K. (2008), "Very simple, carbuncle-free, boundary-layer-resolving, rotated-hybrid Riemann solvers", *J. Comput. Phys.*, **227**, 2560-2581. https://doi.org/10.1016/j.jcp.2007.11.003.

Osher, S. and Solomon, F. (1982), "Upwind difference schemes for hyperbolic systems of conservation laws", *Math. Comput.*, **38**, 339-374.

Pandolfi, M. (1984), "A contribution to the numerical prediction of unsteady flows", *AIAA J.*, **22**, 602-610. https://doi.org/10.2514/3.48491.

Pandolfi, M. and D'Ambrosio, D. (2001), "Numerical instabilities in upwind methods: analysis and cures for the "carbuncle" phenomenon", *J. Comput. Phys.*, **166**, 271-301. https://doi.org/10.1006/jcph.2000.6652.

Peery, K.M. and Imlay, S.T. (1988), "Blunt body flow simulations", *AIAA J.*, 2904. https://doi.org/10.2514/6.1988-2904.

Quirk, J.J. (1992), "A contribution to the great Riemann solver debate", ICASE Report, 92-64.

Rodionov, A.V. (2018), "Development of methods and programs for numerical simulations to non-equilibrium supersonic flows applied to aerospace and astrophysical problems", Research Thesis for the Degree of a Doctor of Physical and Mathematical Sciences, Sarov.

Rodionov, A.V. (2019), "Artificial viscosity to cure the shock instability in high-order Godunov-type schemes", *Comput. Fluid.*, **190**, 77-97. https://doi.org/10.1016/j.compfluid.2019.06.011.

Rodionov, A.V. (2021), "Simplified artificial viscosity approach for curing the shock instability", *Comput. Fluid.*, **219**, 1-17. https://doi.org/10.1016/j.compfluid.2021.104873.

Roe, P., Nishikawa, H., Ismail, F. and Scalabrin, L. (2005), "On carbuncles and other excrescences", *17th AIAA Computational Fluid Dynamics Conference*, 4872.

Roe, P.L. (1981), "Approximate Riemann solvers, parameter vectors, and difference schemes", *J. Comput. Phys.*, **43**, 357-372. https://doi.org/10.1016/0021-9991(81)90128-5.

Rusanov, V.V. (1962), "The calculation of the interaction of non-stationary shock waves and obstacles", *USSR Comput. Math. Math. Phys.*, **1**(2), 304-320.

Spiteri, R.J. and Ruuth, S.J. (2002), "A new class of optimal high-order strong-stability-preserving time discretization methods", *SIAM J. Numer. Anal.*, **40**(2), 469-491. https://doi.org/10.1137/S0036142901389025.

Toro, E.F. (2010), *Riemann Solvers and Numerical Methods for Fluid Dynamics*, Third Edition, Springer.

Woodward, P. and Colella, Ph. (1984), "The numerical simulation of two-dimensional fluid flow with strong shocks", *J. Comput. Phys.*, **54**(1), 115-173. https://doi.org/10.1016/0021-9991(84)90142-6.

Xie, W., Li, W., Li, H., Tian, Z. and Pan, S. (2017), "On numerical instabilities of Godunov-type schemes

for strong shocks", *J. Comput. Phys.*, **350**, 607-637. https://doi.org/10.1016/j.jcp.2017.08.063.
Yasue, K., Furudate, M., Ohnishi, N. and Sawada, K. (2010), "Implicit discontinuous Galerkin method for RANS simulation utilizing pointwise relaxation algorithm", *Commun. Comput. Phys.*,**7**(3), 510-533.